Brain Pathology ISSN 1015-6305

RESEARCH ARTICLE

Intratumoral Heterogeneity of Genomic Imbalance in a Case of Epithelioid Glioblastoma with *BRAF* V600E Mutation

Sumihito Nobusawa[1]; Junko Hirato[2]; Hideyuki Kurihara[3]; Akira Ogawa[4]; Naoki Okura[5]; Masaya Nagaishi[1,6]; Hayato Ikota[1]; Hideaki Yokoo[1]; Yoichi Nakazato[1,7]

[1] Department of Human Pathology, Gunma University Graduate School of Medicine, Maebashi, Japan.
[2] Department of Pathology, Gunma University Hospital, Maebashi, Japan.
[3] Department of Neurosurgery, National Hospital Organization Takasaki General Medical Center, Takasaki, Japan.
[4] Department of Pathology, National Hospital Organization Takasaki General Medical Center, Takasaki, Japan.
[5] Department of Radiology, Graduate School of Medicine, University of Tokyo, Tokyo, Japan.
[6] Department of Neurosurgery, Koshigaya Hospital, Dokkyo University School of Medicine, Koshigaya, Japan.
[7] Department of Pathology, Hidaka Hospital, Takasaki, Japan.

Keywords
array CGH, *BRAF*, epithelioid glioblastoma, LSAMP.

Corresponding author:
Sumihito Nobusawa, MD, Department of Human Pathology, Gunma University Graduate School of Medicine, 3-39-22, Showa-machi, Maebashi, Gunma 371-8511 (E-mail: *nobusawa0319@gunma-u.ac.jp*)

Received 18 November 2013
Accepted 10 December 2013
Published Online Article Accepted 13 December 2013

The authors declare no conflict of interest

doi:10.1111/bpa.12114

Abstract

Epithelioid glioblastoma is among the rarest variants of glioblastoma and is not formally recognized in the World Health Organization classification; it is composed of monotonous, discohesive sheets of small, round cells with eccentric nuclei and eosinophilic cytoplasm devoid of cytoplasmic stellate processes, showing the retention of nuclear staining of INI-1 protein. Here, we report a case involving a 22-year-old man with a right occipital lobe tumor, which comprised mainly epithelioid tumor cells with a small area of diffusely infiltrating less atypical astrocytoma cells showing a lower cell density. Array comparative genomic hybridization separately performed for each histologically distinct component demonstrated eight shared copy number alterations (CNAs) and three CNAs observed only in epithelioid cells; one of the latter was a homozygous deletion of a tumor suppressor gene, *LSAMP*, at 3q13.31. *BRAF* V600E mutation was observed both in epithelioid tumor cells and in diffusely infiltrating less atypical astrocytoma cells. Our findings suggest that the regional loss of *LSAMP* led to the aggressive nature of epithelioid cells in the present case of epithelioid glioblastoma.

INTRODUCTION

Glioblastoma, the highest-grade tumor in the spectrum of diffusely infiltrating astrocytic neoplasms, is morphologically heterogeneous and harbors a great variety of genetic alterations. Various histological subtypes are recognized, including giant cell, gemistocytic, small cell and granular cell forms (13).

Epithelioid glioblastoma is among the rarest variants of glioblastoma, and is not formally recognized in the World Health Organization (WHO) classification of the central nervous system (CNS) tumors (13–15). Epithelioid glioblastomas are composed of monotonous, patternless sheets of small, round cells with laterally positioned nuclei and eosinophilic cytoplasm (15). Although epithelioid glioblastomas share similar histological features with rhabdoid glioblastomas, and these terms have been used interchangeably in previously published reports (2, 10, 18, 21, 28), Kleinschmidt-DeMasters *et al* proposed that polyphenotypic immunohistochemical expression and focal loss of INI-1 protein in the rhabdoid areas should differentiate rhabdoid glioblastomas from epithelioid glioblastomas (13). Clinically, epithelioid glioblastomas tend to occur in the first three decades of life, and the prognosis seems to be poorer than in ordinary glioblastomas (4, 14).

BRAF V600E mutation has been found commonly in certain CNS tumors, including pleomorphic xanthoastrocytomas (PXA) (60%), PXA with anaplastic features (60%), gangliogliomas (20%–60%), and extracerebellar pilocytic astrocytomas (20%) (6, 8, 16, 31). Recently, *BRAF* V600E mutation was also found in epithelioid glioblastomas at the relatively high frequency of 54% (7/13 cases) (14).

In the same series of epithelioid glioblastoma reported by Kleinschmidt-DeMasters *et al*, except for a single case of secondary epithelioid glioblastoma with *IDH1* mutation, a molecular signature of the common type of secondary glioblastomas, which progressed from oligoastrocytoma WHO grade II, the others were clinically primary/*de novo* epithelioid glioblastomas and none of them were positive for *IDH1* mutation (14). However, original imaging reports of some primary cases with *BRAF* V600E mutation suggested preexisting low-grade or long-standing tumors, despite the fact that possible precursor lesions could not be identified in the resected specimens (14).

In this report, we present a case of primary epithelioid glioblastoma with small areas either of diffusely infiltrating less atypical astrocytoma cells with a lower cell density or spindle cells. We investigated genetic associations among the histologically distinct tumor cells, performing molecular and cytogenetic analyses separately for each component.

MATERIALS AND METHODS

Case history

A 22-year-old man presented with headache. Magnetic resonance imaging (MRI) showed subcortical hemorrhage in the right occipital lobe, and the patient was treated with conservative management. The first follow-up MRI at 4 months showed enlargement of the hematoma without clear evidence of a tumor; however, the second follow-up MRI at 6 months disclosed a heterogenously enhanced mass with hemorrhagic components and prominent surrounding edema in the right occipital lobe (Figure 1). A subtotal resection of the mass was then performed. After establishing a diagnosis, extended focal radiotherapy and chemotherapy with temozolomide and interferon-beta were delivered. From 5 months after surgery, local recurrence, extensive dissemination in the intracranial and spinal subarachnoid space, and metastases to vertebral bodies, the right thoracic wall, right lung and liver were found consecutively. Palliative radiotherapy was appropriately administered, and the patient was still alive 24 months after the diagnosis. This study was approved by the Ethics Committee of Gunma University.

Conventional histological analysis

Tumor sections were fixed with 10% formalin and embedded in paraffin. Three-micrometer-thick tissue sections were cut and stained with hematoxylin and eosin (H&E). Some sections were double-stained with H&E and periodic acid-methenamine silver. Immunohistochemical staining was performed on formalin-fixed, paraffin-embedded sections. Four primary antibodies directed against the following antigens were applied: glial fibrillary acidic protein (GFAP) (1:5000) (24), Olig2 (1:5000) (37), vimentin (V9; 1:200; Dako, Glostrup, Denmark), cytokeratin (CAM5.2; 1:5; BD Bioscience, San Jose, CA, USA), BAF47/INI1 (BAF47; 1:100; BD Bioscience) and Ki-67 (MIB-1; 1:100; Dako). For coloration, a commercially available biotin-streptavidin immunoperoxidase kit (Histofine, Nichirei, Tokyo, Japan) and diaminobenzidine were employed.

DNA extraction

DNA was extracted from paraffin-embedded sections separately from an area with epithelioid tumor cells, an area of less atypical astrocytoma cells with a lower cell density and a spindle cell area, as previously described (12, 26).

Array comparative genomic hybridization (CGH)

Array CGH analysis was carried out using a 4×180 K CGH oligonucleotide microarray (AgilentTechnologies, Santa Clara, CA, USA), as described previously (12, 26). The log2 ratio of <-1.0 at the region of interest was considered to represent homozygous deletion, and a value of -1.0 to -0.2 was considered to represent heterozygous deletion (32).

Differential polymerase chain reaction (PCR)

A search for homozygous deletion in intron 3 of the *LSAMP* gene was carried out employing differential PCR, as previously reported (29), using two primer sets (fragments #1 and #2) located in intron 3 of the *LSAMP* gene with the *CF* gene sequence as a reference (33). The primer sequences were as follows: 5′-AAC AGG CCG TGA ATA AAC ACA-3′ (sense) and 5′-ACC AAA TGC GGA TGA ATA GAG A-3′ (antisense) for fragment #1 (PCR product, 110 bp), and 5′-CAA TGG ATA GGC AAA ATC AGG A-3′ (sense) and 5′-TTC AAG CCT TGT TGC TTG CTT-3′ (antisense) for fragment #2 (PCR product, 105 bp). The mean signal ratio of fragments #1 and #2 to *CF* of normal DNA (14 non-tumoral tissues from healthy individuals) was 0.96 and 0.98, with standard

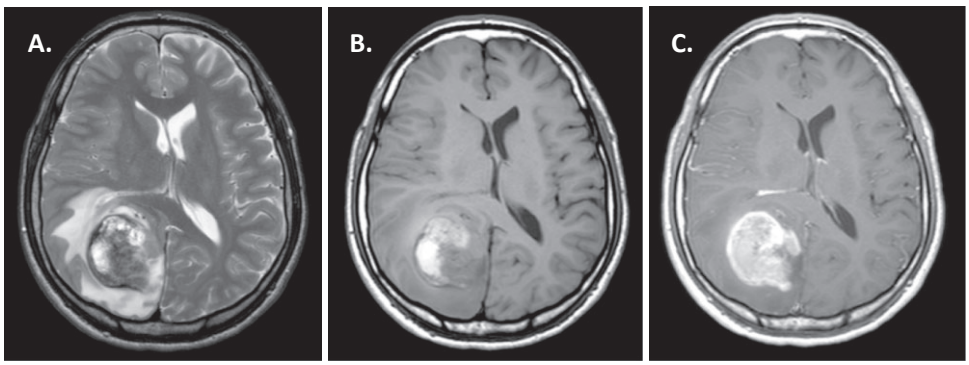

Figure 1. *Magnetic resonance imaging.* **A.** Axial T2-weighted images demonstrated a heterogenous mass with high-low signal intensity measuring 50 mm in the right occipital lobe. Prominent peritumoral edema and midline shift were seen. **B.** On axial T1-weighted images, heterogenous high signal intensity suggesting a hemorrhagic component was seen. **C.** Axial gadolinium-enhanced T1-weighted images showed homogeneous enhancement with strong ring-like enhancement.

variations of 0.16 and 0.10, respectively. Samples with a ratio of ≤0.2 were considered to show homozygous deletion (23).

Fluorescence *in situ* hybridization (FISH) analysis

Dual-probe hybridization using an intermittent microwave irradiation method was applied to paraffin-embedded, 4-μm-thick tissue sections, as described previously (36). A 4q34.3–4q35.1 probe was prepared from a bacterial artificial chromosome (BAC) clone, RP11-713O21, labeled with ENZO Orange-dUTP (Abbott Molecular Inc., Des Plaines, IL, USA), and a 4p15.2 probe was prepared from a BAC clone RP11–758 M15 labeled with ENZO Green-dUTP (Abbott Molecular Inc.).

Reverse transcription (RT)-differential PCR

An RNeasy FFPE kit (Qiagen, Hilden, Germany) was used to isolate total RNA from paraffin-embedded sections, separately from an area with epithelioid tumor cells and from an area of diffusely infiltrating less atypical astrocytoma cells with a lower cell density. First-strand cDNA was synthesized from total RNA using the SuperScript VILO cDNA Synthesis Kit (Life Technologies Carlsbad, CA, USA). Then, differential PCR was performed as previously reported (11), using a primer set covering exon boundary 3–4 of the *LSAMP* mRNA with the *GAPDH* mRNA sequence as a reference (20). The primer sequences were as follows: 5′-CCT GAA CCT GTT ATC ACC TGG A-3′ (sense) and 5′-GAC CTC GTT GGC AGC TTT G-3′ (antisense) for *LSAMP* (PCR product, 135 bp). Human brain-derived BioBank cDNA (PrimerDesign, Southampton, UK) was used as a normal control.

Direct DNA sequencing for *BRAF* and *IDH1/2* mutations

Genomic DNA separately extracted from an area with epithelioid tumor cells and a small area of diffusely infiltrating less atypical astrocytoma cells with a lower cell density was amplified by PCR using primers for exon 15 of the *BRAF* gene and exon 4 of the *IDH1* and *IDH2* genes. The primer sequences were previously reported (1, 31, 34). PCR products were sequenced on a 3130xl Genetic Analyzer (Applied Biosystems, Foster City, CA, USA) with the Big Dye Terminator v.1.1 Cycle Sequencing Kit (Applied Biosystems) following standard procedures.

RESULTS

Pathological findings

On histopathologic examination, the tumor was composed mainly of discohesive sheets of medium-sized, uniform cells with round cytoplasmic contours and eosinophilic cytoplasm devoid of cytoplasmic stellate processes (Fig 2A,B). The nuclei were large, mostly eccentric, and variable in shape: round, ovoid, reniform, crescent or ring-like (Figure 2B). The cells often had less defined hyalinized cytoplasmic inclusions, some of which contained fine basophilic granules (Figure 2B). Small cytoplasmic vacuoles were also found in some tumor cells. Multiple mitotic figures were found. Interspersed neuropil was absent (Figure 2B). Prominent hemorrhage and extensive coagulative necrosis were seen (Figure 2C left). Microvascular proliferation was absent. Tumor-cell invasion into the vascular wall was observed (Figure 2C right). These characteristics are consistent with the descriptions of epithelioid glioblastoma by Kleinschmidt-DeMasters *et al* (13, 14). These epithelioid tumor cells accounted for more than 90% of the tumor tissue.

In addition, a small area of the tumor displayed the proliferation of well-differentiated neoplastic fibrillary astrocytes in the background of a loosely structured matrix (Figure 2D,E). Histological features of pilocytic astrocytoma or pleomorphic xanthoastrocytoma, such as bipolar piloid processes, a microcystic structure, cellular pleomorphism, Rosenthal fibers or eosinophilic granular bodies, were not obvious. Mitotic figures were absent.

Furthermore, another small part of the tumor extending within the subarachnoid space showed spindle-shaped cells (Figure 2F). These cells had discernible nucleoli, and three mitoses were detected in 10 high-power fields.

GFAP immunoreactivity was identified in a limited number of epithelioid cells (Figure 3A), but was diffusely obserbed in less atypical astrocytoma cells (Figure 3B). The cytoplasm of epithelioid cells showed diffuse and strong staining with vimentin (Figure 3C). Nuclear Olig2 staining was noted only in a small number of epithelioid cells (Figure 3D). Cytoplasmic immunostaining of cytokeratin CAM5.2 was not identified in epithelioid cells (Figure 3E). The retention of nuclear staining of INI-1 was observed throughout the specimen (Figure 3F). MIB-1 labeling indexes of epithelioid tumor cells, less atypical astrocytoma cells with a lower cell density, and spindle tumor cells were 22.6%, 2.4% and 8.3%, respectively.

Array CGH

Array CGH showed 11 copy number alterations (CNAs). Eight CNAs were detected in all three histological areas analyzed (Table 1), while the others (a homozygous deletion in *LSAMP*, a heterozygous deletion in *ODZ3*, and a heterozygous deletion in *LRP1B*) were found only in epithelioid tumor cells (Figure 4A–C). The homozygous deletion in *LSAMP* was in intron 3, and its size was 43 kb.

Validation of array CGH data

Differential PCR was carried out to assess the homozygous deletion in intron 3 of the *LSAMP* gene, which was detected by array CGH, in epithelioid tumor cells and diffusely infiltrating less atypical astrocytoma cells using two primer sets (fragments #1 and #2), and the deletion was confirmed in epithelioid tumor cells (Figure 4A).

FISH analysis was carried out to assess the heterozygous deletion in *ODZ3*, which was detected by array CGH, in epithelioid tumor cells and less atypical astrocytoma cells, and the deletion was revealed only in epithelioid tumor cells (Figure 4B).

LSAMP mRNA expression

RT-differential PCR detected *LSAMP* mRNA expression in a small area of diffusely infiltrating less atypical astrocytoma cells (28% reduction compared with normal control), but the expression was

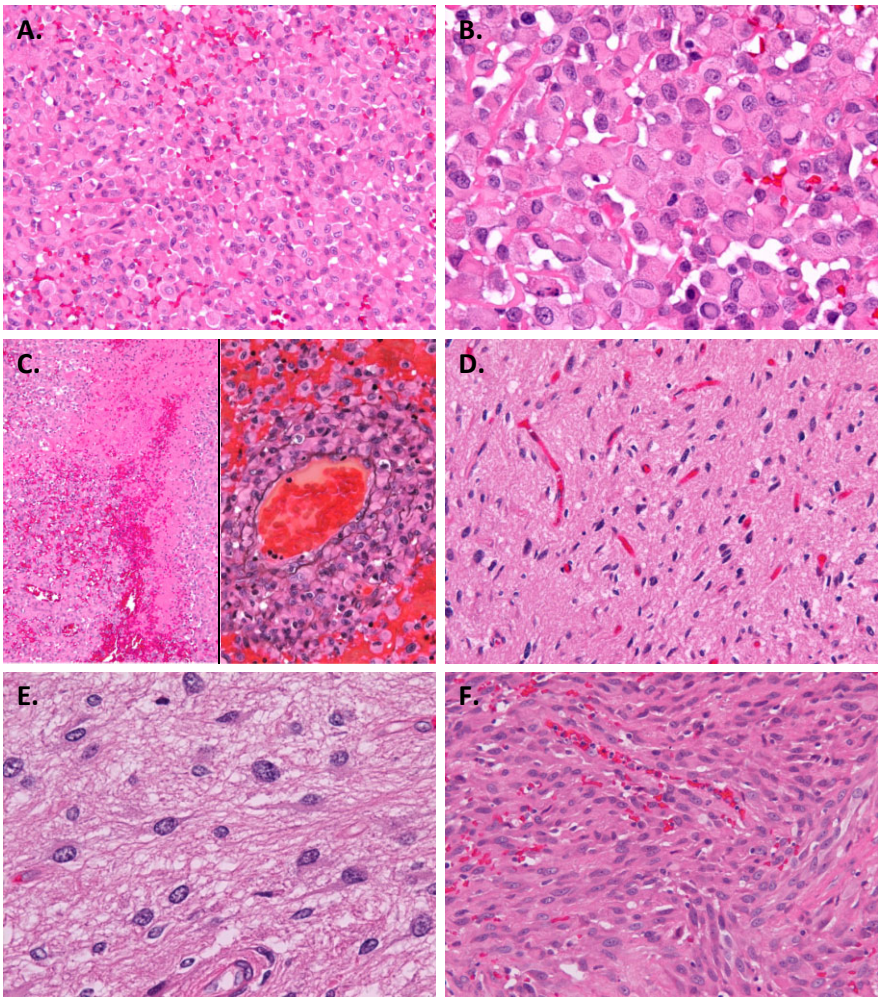

Figure 2. *Microscopic appearance.* **A.** The tumor was composed mainly of discohesive sheets of medium-sized uniform cells. **B.** The tumor cells had rounded cytoplasmic contours and eosinophilic cytoplasm. The nuclei were large and mostly eccentric, and variable in shape: round, ovoid, reniform, crescent or ring-like. The cells often had hyalinized cytoplasmic inclusions, some of which contained fine basophilic granules. **C.** Hemorrhage and coagulative necrosis (left). Tumor-cell invasion into the vascular wall demonstrated by staining with both hematoxylin and eosin and periodic acid-methenamine silver (right). **D**, **E.** A small area of the tumor displayed the proliferation of well-differentiated neoplastic fibrillary astrocytes. **F.** A small part of the tumor extending within the subarachnoid space showed spindle-shaped cells. Original magnification: ×100 (**C** left), ×200 (**A**, **C** right, **D**, **F**), ×400 (**B**, **E**).

below the detection limit in an area with epithelioid tumor cells (Figure 4A).

BRAF and *IDH1/2* mutations

The heterozygous *BRAF* V600E mutation was found both in an area with epithelioid tumor cells and in a small area of diffusely infiltrating less atypical astrocytoma cells (Figure 5). No mutation in exon 4 of *IDH1* and *IDH2* was observed in either area analyzed (data not shown).

DISCUSSION

In the current study, array CGH was performed separately for epithelioid tumor cells, which accounted for the majority of the tumor, a small area of diffusely infiltrating less atypical astrocytoma cells with a lower cell density, and a spindle cell area in a single case of epithelioid glioblastoma. The results demonstrated that 8 of 11 CNAs were identical in all tumor areas analyzed (Table 1, Figure 4D). Among 3 CNAs specific to epithelioid tumor cells, we focused on the only homozygously deleted gene, that is, *LSAMP* at 3q13.31. Deletion of *LSAMP* has been reported to be involved in tumorgenesis (5, 17, 27, 35). The *LSAMP* gene has been established as a tumor suppressor gene, which was frequently deleted, down-regulated or epigenetically silenced in osteosarcoma and renal cell carcinoma (5, 17, 27, 35). Recent data from The Cancer Genome Atlas, analyzing 578 samples of glioblastoma, showed infrequent single gene deletion involving *LSAMP* (3). In the present report, a homozygous deletion of *LSAMP* found in epithelioid cells was detected in an intron, but was shown to lead to a loss of *LSAMP* mRNA expression (Figure 4A). Taken together, the possibility cannot be ruled out that the regional loss of *LSAMP* led to the aggressive nature of epithelioid cells in the present case. Moreover, whether or not the inactivation of *LSAMP* is a frequent event in this rare type of glioblastoma needs to be further investigated. The other hemizygously deleted genes, *ODZ3* and *LRP1B* were also reported to be potent tumor supressor genes (7, 19, 22, 25), and their biological significance in tumorigenesis requires further investigation as well.

Along with PXA, gangliogliomas and extracerebellar pilocytic astrocytomas, frequent *BRAF* V600E mutation was also reported in epithelioid glioblastomas (14). In the present case, *BRAF* V600E mutation was observed not only in an area with epithelioid tumor cells, but also in an area of less atypical astrocytoma cells

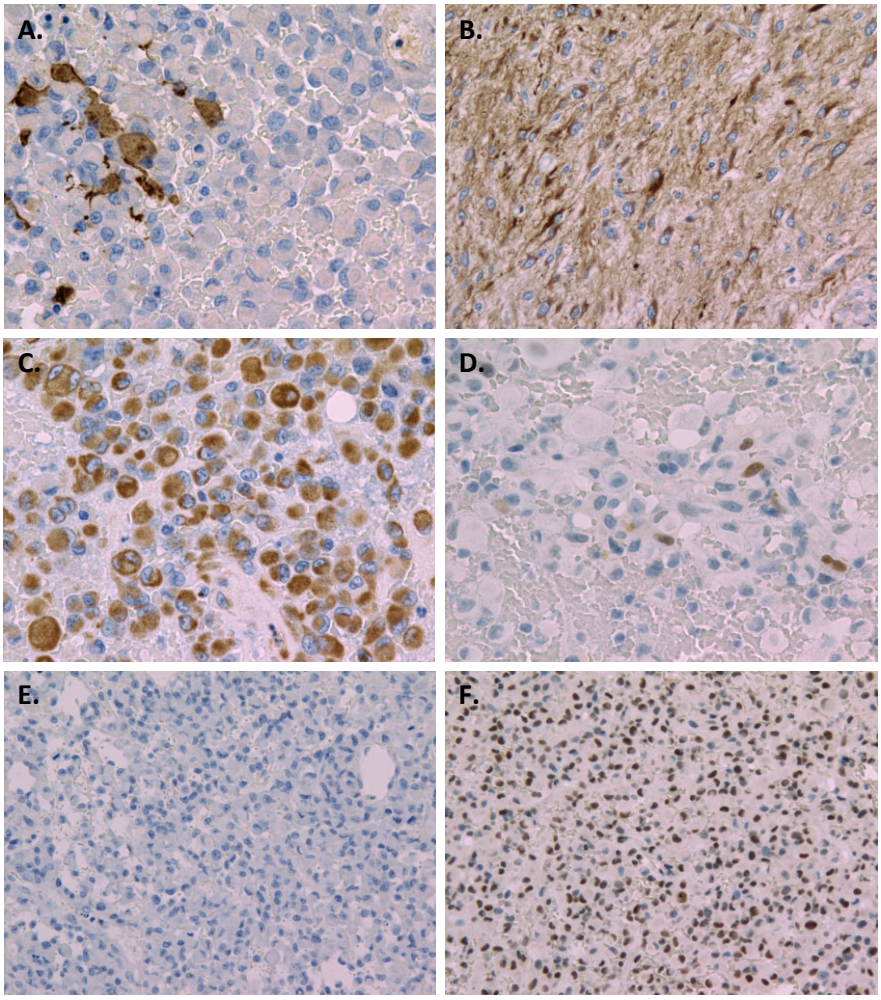

Figure 3. *Immunohistochemistry.* Glial fibrillary acidic protein immunoreactivity was identified in a limited number of epithelioid cells (**A**), but was diffusely observed in less atypical astrocytoma cells (**B**). **C.** Diffuse and strong vimentin staining was seen in the cytoplasm of epithelioid cells. **D.** Nuclear Olig2 staining was found only in a small number of epithelioid cells. **E.** Cytoplasmic immunostaining of CAM5.2 was not identified in epithelioid cells. **F.** Retention of nuclear staining of INI-1 was observed in epthelioid tumor cells. Original magnification: ×200 (**D**, **E**, **F**), ×400 (**A**, **B**, **C**).

with a lower cell density (Figure 5), which may mean that the acquisition of the *BRAF* mutation occurred at tumor initiation. Concurrent *BRAF* V600E mutation and *CDKN2A* homozygous deletion have been found in a subset of diffuse astrocytomas without *IDH1/2* mutations in children and young adults (9, 30). This combination of alterations, which was observed in the present case (Table 1, Figure 4D), has also been detected in astrocytic tumors of higher malignancy grades in the same age category (30).

The present case showed extensive systemic spread including dissemination in the intracranial and spinal subarachnoid space,

Table 1. Abberations common to all histological areas analyzed by array comparative genomic hybridazation.

Chromosomal location	Loc. Start*	Loc. Stop*	Length (Kb)	Aberration**	Gene names
3q26.1	162514534	162619141	104.6	Deletion (–1.849218)	
4q13.2	69392545	69462438	69.9	Deletion (–1.831354)	*UGT2B17, UGT2B15*
6p22.1	29854870	29896710	41.8	Deletion (–1.236831)	*HLA-H, HCG2P7, HCG4P6*
8p11.22	39237438	39345479	108.0	Amplification (0.671442)	*ADAM5P, ADAM3A*
9p21.3	21944037	22176231	232.2	Deletion (–1.62978)	*C9orf53, CDKN2A, CDKN2BAS, CDKN2B*
15q11.1–q11.2	20575646	21933378	1357.7	Amplification (0.937772)	*GOLGA6L6, GOLGA8C, BCL8, POTEB, NF1P1, LOC646214*
20p12.1	14903016	15015311	112.3	Deletion (–0.880196)	*MACROD2*
22q11.23	24347959	24390254	42.3	Deletion (–1.449985)	*LOC391322, GSTT1, GSTTP2*

Loc. = location on chromosame.

*Genome mapping based on genome build hg19.

**The numbers in parentheses are the average log2 ratio of each aberration.

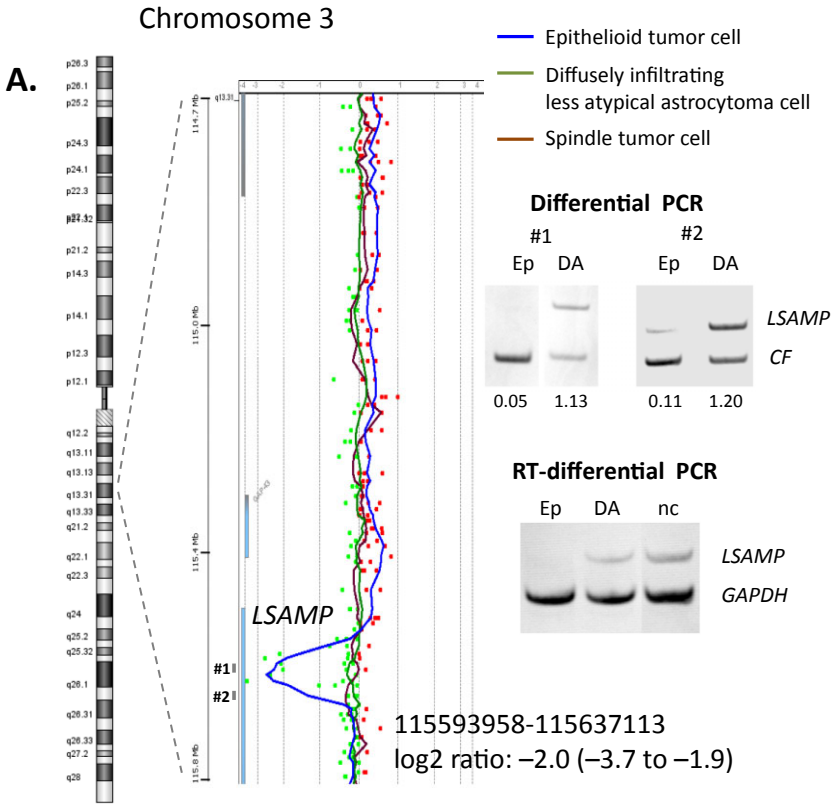

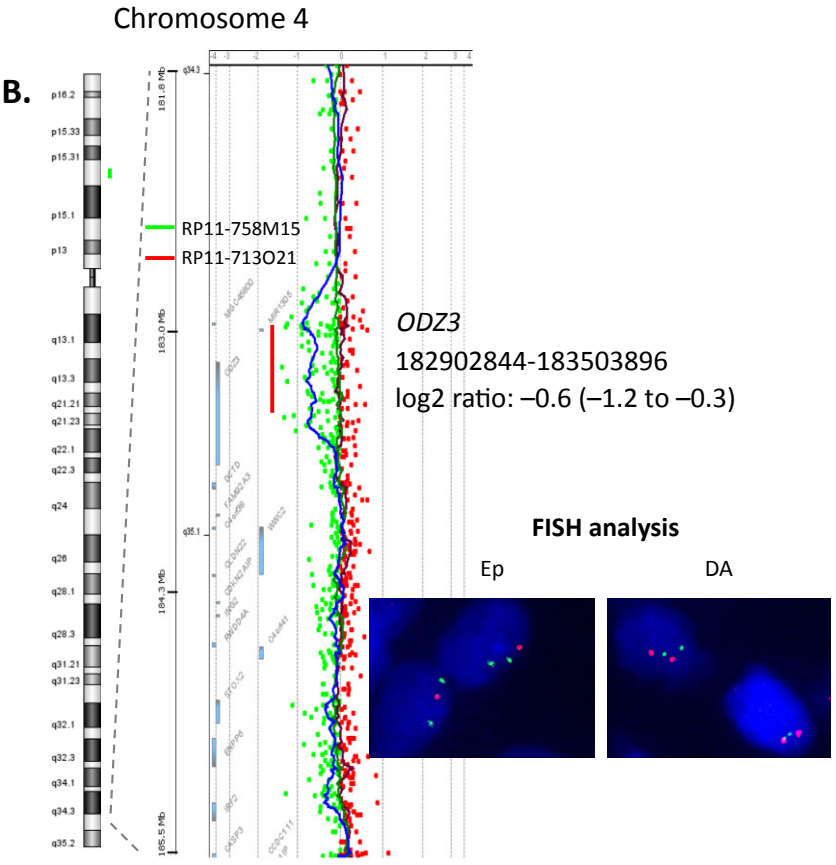

Figure 4. Three aberrations found only in epithelioid tumor cells (**A**–**C**) and one example of aberrations detected in all histological areas (**D**) by array CGH. **A.** A homozygous deletion in intron 3 of the *LSAMP*. The deletion was validated by differential PCR using two primer sets (fragments #1 and #2) located in the deleted part shown by array CGH. Numbers below each band of differential PCR indicate the ratio of amplification of the target compared with the *CF* reference gene. RT-differential PCR showed *LSAMP* mRNA expression in diffusely infiltrating less atypical astrocytoma cells but not in epithelioid tumor cells. #1, 2 = fragments #1, 2. **B.** A heterozygous deletion in *ODZ3*. The deletion was validated by FISH analysis. BAC clones used for the target (RP11-713O21; 4q34.3–4q35.1) and reference (RP11–758 M15; 4p15.2) probes are indicated with red and green bars, respectively. **C.** A heterozygous deletion in *LRP1B*. **D.** A homozygous deletion in *CDKN2A/2B*. Abbreviations: BAC = bacterial artificial chromosome; CGH = comparative genomic hybridization; DA = diffusely infiltrating less atypical astrocytoma cells; Ep = epithelioid tumor cells; FISH = fluorescence *in situ* hybridization; nc = normal control; PCR = polymerase chain reaction; RT = reverse transcription.

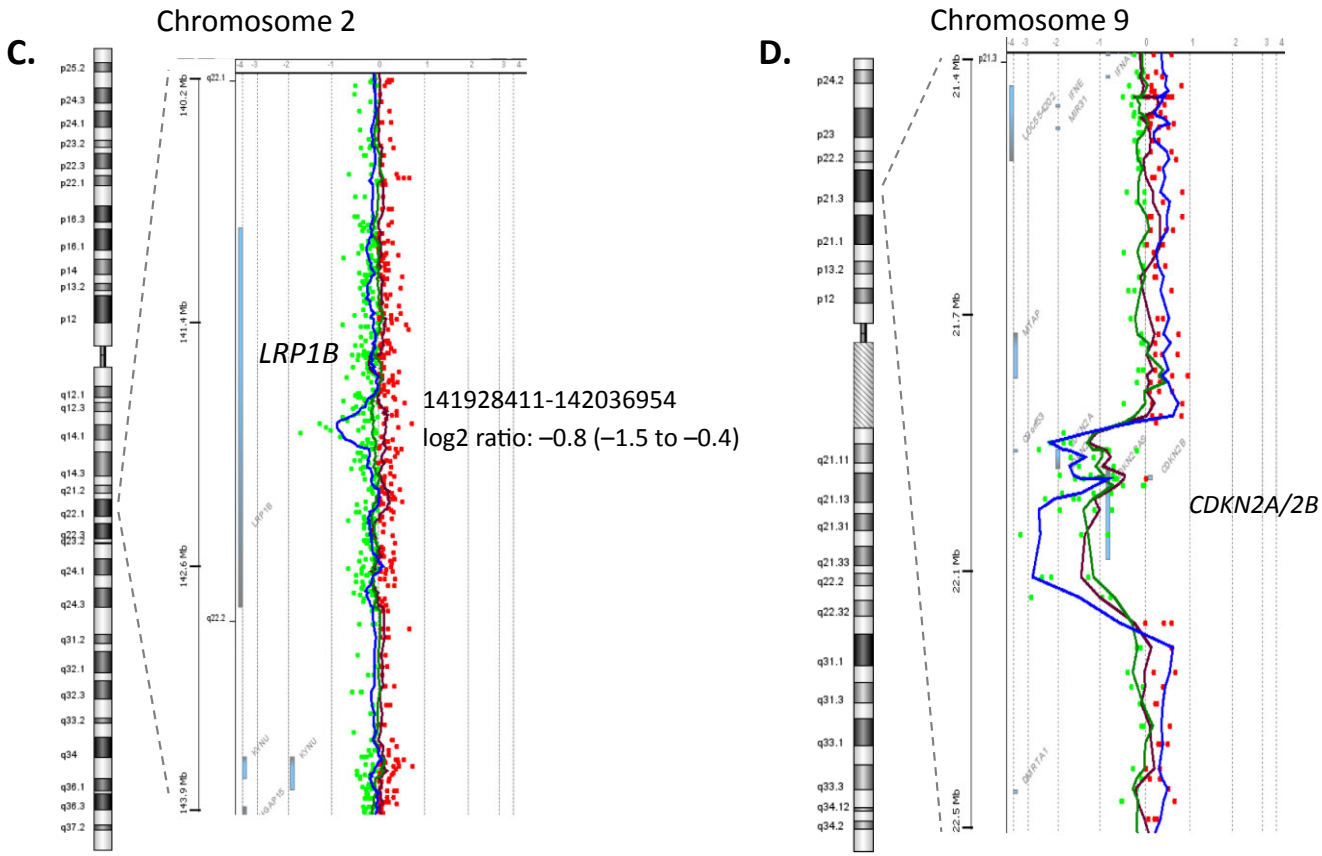

Figure 4. *Continued*

and metastases to vertebral bodies, the right thoracic wall, right lung and liver. Some epithelioid glioblastomas have reported to show cerebrospinal fluid dissemination and/or disease progression at sites outside the CNS: peritoneal tumor deposites and multiple liver metastases (4, 14, 15). These behaviors are not typical of conventional glioblastomas (13), but seem not to be infrequent in epithelioid glioblastomas.

In conclusion, our results suggest that the regional loss of *LSAMP* led to the aggressive nature of epithelioid cells in the present case of epithelioid glioblastoma. Large cohorts will have to be tested to explore additional pathobiologic and prognostic differences associated with epithelioid glioblastomas.

ACKNOWLEDGMENTS

We thank Ms. Machiko Yokota and Mr. Koji Isoda (Gunma University) for their excellent technical assistance.

REFERENCES

1. Arai M, Nobusawa S, Ikota H, Takemura S, Nakazato Y (2012) Frequent IDH1/2 mutations in intracranial chondrosarcoma: a possible diagnostic clue for its differentiation from chordoma. *Brain Tumor Pathol* **29**:201–206.
2. Babu R, Hatef J, McLendon RE, Cummings TJ, Sampson JH, Friedman AH, Adamson C (2013) Clinicopathological characteristics and treatment of rhabdoid glioblastoma. *J Neurosurg* **119**:412–419.

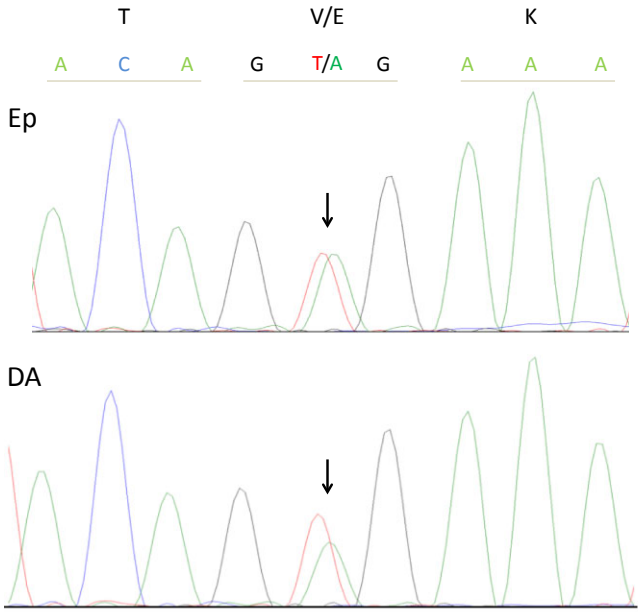

Figure 5. Illustration of the heterozygous *BRAF* V600E mutation (arrow) found in both an area with epithelioid tumor cells (upper) and an area of diffusely infiltrating less atypical astrocytoma cells (lower).

3. Brennan CW, Verhaak RG, McKenna A, Campos B, Noushmehr H, Salama SR *et al* (2013) The somatic genomic landscape of glioblastoma. *Cell* **155**:462–477.
4. Broniscer A, Tatevossian RG, Sabin ND, Klimo P Jr, Dalton J, Lee R *et al* (2013) Clinical, radiological, histological, and molecular characteristics of paediatric epithelioid. *Neuropathol Appl Neurobiol* doi: 10.1111/nan.12093.
5. Chen J, Lui WO, Vos MD, Clark GJ, Takahashi M, Schoumans J *et al* (2003) The t(1;3) breakpoint-spanning genes LSAMP and NORE1 are involved in clear cell renal cell carcinoma. *Cancer Cell* **4**:405–413.
6. Dias-Santagata D, Lam Q, Vernovsky K, Vena N, Lennerz JK, Borger DR *et al* (2011) *BRAF* V600E mutations are common in pleomorphic xanthoastrocytoma: diagnostic and therapeutic. *PLoS ONE* **6**:e17948.
7. Ding L, Getz G, Wheeler DA, Mardis ER, McLellan MD, Cibulskis K *et al* (2008) Somatic mutations affect key pathways in lung adenocarcinoma. *Nature* **455**:1069–1075.
8. Dougherty MJ, Santi M, Brose MS, Ma C, Resnick AC, Sievert AJ *et al* (2010) Activating mutations in *BRAF* characterize a spectrum of pediatric low-grade gliomas. *Neuro-Oncol* **12**:621–630.
9. Forshew T, Tatevossian RG, Lawson AR, Ma J, Neale G, Ogunkolade BW *et al* (2009) Activation of the ERK/MAPK pathway: a signature genetic defect in posterior fossa pilocytic astrocytomas. *J Pathol* **218**:172–181.
10. He MX, Wang JJ (2011) Rhabdoid glioblastoma: case report and literature review. *Neuropathology* **31**:421–426.
11. Huang H, Colella S, Kurrer M, Yonekawa Y, Kleihues P, Ohgaki H (2000) Gene expression profiling of low-grade diffuse astrocytomas by cDNA arrays. *Cancer Res* **60**:6868–6874.
12. Kim YH, Lachuer J, Mittelbronn M, Paulus W, Brokinkel B, Keyvani K *et al* (2011) Alterations in the RB1 pathway in low-grade diffuse gliomas lacking common genetic alterations. *Brain Pathol* **21**:645–651.
13. Kleihues P, Burger PC, Aldape KD, Brat DJ, Biernat W, Bigner DD (2007) Glioblastoma. Chapter 1. In: *WHO Classification of Tumours of the Central Nervous System*. DN Louis, H Ohgaki, OD Wiestler, WK Cavenee (eds), pp. 33–59. IARC Press: Lyon.
14. Kleinschmidt-DeMasters BK, Aisner DL, Birks DK, Foreman NK (2013) Epithelioid GBMs show a high percentage of *BRAF* V600E mutation. *Am J Surg Pathol* **37**:685–698.
15. Kleinschmidt-DeMasters BK, Alassiri AH, Birks DK, Newell KL, Moore W, Lillehei KO (2010) Epithelioid versus rhabdoid glioblastomas are distinguished by monosomy 22 and immunohistochemical expression of INI-1 but not claudin 6. *Am J Surg Pathol* **34**:341–354.
16. Koelsche C, Wöhrer A, Jeibmann A, Schittenhelm J, Schindler G, Preusser M *et al* (2013) Mutant *BRAF* V600E protein in ganglioglioma is predominantly expressed by neuronal tumor cells. *Acta Neuropathol* **125**:891–900.
17. Kresse SH, Ohnstad HO, Paulsen EB, Bjerkehagen B, Szuhai K, Serra M *et al* (2009) LSAMP, a novel candidate tumor suppressor gene in human osteosarcomas, identified by array comparative genomic hybridization. *Genes Chromosomes Cancer* **48**:679–693.
18. Lath R, Unosson D, Blumbergs P, Stahl J, Brophy BP (2003) Rhabdoid glioblastoma: a case report. *J Clin Neurosci* **10**:325–328.
19. Letouzé E, Rosati R, Komechen H, Doghman M, Marisa L, Flück C *et al* (2012) SNP array profiling of childhood adrenocortical tumors reveals distinct pathways of tumorigenesis and highlights candidate driver genes. *J Clin Endocrinol Metab* **97**:E1284–E1293.
20. Lv SQ, Kim YH, Giulio F, Shalaby T, Nobusawa S, Yang H *et al* (2012) Genetic alterations in microRNAs in medulloblastomas. *Brain Pathol* **22**:230–239.
21. Momota H, Iwami K, Fujii M, Motomura K, Natsume A, Ogino J *et al* (2011) Rhabdoid glioblastoma in a child: case report and literature review. *Brain Tumor Pathol* **28**:65–70.
22. Nagayama K, Kohno T, Sato M, Arai Y, Minna JD, Yokota J (2007) Homozygous deletion scanning of the lung cancer genome at a 100-kb resolution. *Genes Chromosomes Cancer* **46**:1000–1010.
23. Nakamura M, Watanabe T, Klangby U, Asker C, Wiman K, Yonekawa Y *et al* (2001) P14Arf deletion and methylation in genetic pathways to glioblastomas. *Brain Pathol* **11**:159–168.
24. Nakazato Y, Ishizeki J, Takahashi K, Yamaguchi H, Kamei T, Mori T (1982) Localization of S-100 protein and glial fibrillary acidic protein-related antigen in pleomorphic adenoma of the salivary glands. *Lab Invest* **46**:621–626.
25. Nikolaev SI, Rimoldi D, Iseli C, Valsesia A, Robyr D, Gehrig C *et al* (2011) Exome sequencing identifies recurrent somatic MAP2K1 and MAP2K2 mutations in melanoma. *Nat Genet* **44**:133–139.
26. Nobusawa S, Lachuer J, Wierinckx A, Kim YH, Huang J, Legras C *et al* (2010) Intratumoral patterns of genomic imbalance in glioblastomas. *Brain Pathol* **20**:936–944.
27. Pasic I, Shlien A, Durbin AD, Stavropoulos DJ, Baskin B, Ray PN *et al* (2010) Recurrent focal copy-number changes and loss of heterozygosity implicate two noncoding RNAs and one tumor suppressor gene at chromosome 3q13.31 in osteosarcoma. *Cancer Res* **70**:160–171.
28. Pimentel J, Silva R, Pimentel T (2003) Primary malignant rhabdoid tumors of the central nervous system: considerations about two cases of adulthood presentation. *J Neurooncol* **61**:121–126.
29. Rollbrocker B, Waha A, Louis DN, Wiestler OD, von Deimling A (1996) Amplification of the cyclin-dependent kinase 4 (CDK4) gene is associated with high cdk4 protein levels in glioblastoma multiforme. *Acta Neuropathol* **92**:70–74.
30. Schiffman JD, Hodgson JG, VandenBerg SR, Flaherty P, Polley MY, Yu M *et al* (2010) Oncogenic *BRAF* mutation with CDKN2A inactivation is characteristic of a subset of pediatric astrocytomas. *Cancer Res* **70**:512–519.
31. Schindler G, Capper D, Meyer J, Janzarik W, Omran H, Herold-Mende C *et al* (2011) Analysis of *BRAF* V600E mutation in 1320 nervous system tumors reveals high mutation frequencies in pleomorphic xanthoastrocytoma, ganglioglioma and extra-cerebellar pilocytic astrocytoma. *Acta Neuropathol* **121**:397–405.
32. Tagawa H, Karnan S, Suzuki R, Matsuo K, Zhang X, Ota A *et al* (2005) Genome-wide array-based CGH for mantle cell lymphoma: identification of homozygous deletions of the proapoptotic gene BIM. *Oncogene* **24**:1348–1358.
33. Tohma Y, Gratas C, Biernat W, Peraud A, Fukuda M, Yonekawa Y *et al* (1998) PTEN (MMAC1) mutations are frequent in primary glioblastomas (*de novo*) but not in secondary glioblastomas. *J Neuropathol Exp Neurol* **57**:684–689.
34. Watanabe T, Nobusawa S, Kleihues P, Ohgaki H (2009) IDH1 mutations are early events in the development of astrocytomas and oligodendrogliomas. *Am J Pathol* **174**:1149–1153.
35. Yen CC, Chen WM, Chen TH, Chen WY, Chen PC, Chiou HJ *et al* (2009) Identification of chromosomal aberrations associated with disease progression and a novel 3q13.31 deletion involving LSAMP gene in osteosarcoma. *Int J Oncol* **35**:775–788.
36. Yokoo H, Kinjo S, Hirato J, Nakazato Y (2006) Fluorescence *in situ* hybridization targeted for chromosome 1p of oligodendrogliomas (in Japanese). *Rinsho Kensa* **50**:761–766.
37. Yokoo H, Nobusawa S, Takebayashi H, Ikenaka K, Isoda K, Kamiya M *et al* (2004) Anti-human Olig2 antibody as a useful immunohistochemical marker of normal oligodendrocytes and gliomas. *Am J Pathol* **164**:1717–1725.